

Detection of short period intensity oscillations in the solar corona observed during the total solar eclipse of august 11, 1999

R Rezaei¹, J Singh², R Cowsik², R Sirinivasan² and A K Saxena²

1. Institute for Advanced Studies in Basic Sciences (IASBS), Zanjan, Iran¹

2. Indian Institute for Astrophysics (IIA), 560034, Bangalore, India

(Received : 20 October 2003. ; in final form 4 May 2004)

Abstract

An experiment to search for short-period intensity oscillations in the solar corona was conducted during the total solar eclipse of August 11, 1999 in Esfahan, Iran. The intensity in the continuum, centered about 4700 Å and with a passband having a half-width of 190 Å, was recorded at a counting rate of 5 Hz using six low-noise Hamamatsu R647 photomultiplier tubes. We recorded intensity values from 6 different regions on the image of the solar corona from 1.2 R_☉ to 1.5 R_☉. The power spectrum analysis of all channels, except for a channel that failed to receive any coronal light, shows excess power in the frequency range 0.02-0.2 Hz. The results of analyzing all channels demonstrate various waves with some degree of coherence and amplitudes from 0.3 to 0.7 percent of the mean coronal brightness. There are some similarities between waves in various channels and it may show that these waves exist in a large region of the corona, of the order of a few hundred thousand kilometers, much larger than the fiber optic diaphragms. The energy flux of each wave was calculated by assuming them as the slow or fast mode waves for the active and quiet regions of the solar corona. The energy flux of the fast mode waves in the active regions is comparable with the required energy flux for heating up the solar corona. The intensity oscillations observed in this experiment are similar to those detected during the 1995 and 1997 eclipses.

Keywords: the sun, corona, coronal heating, eclipse

1. Introduction

The fact that the solar corona is at a temperature in excess of 10⁶ K has been known for over half a century. Of course, there are various kinds of temperatures, such as ionization temperature, line-width temperature, and radio brightness temperature. Among them, the ionization temperature is determined more accurately than the others [1]. These temperatures are not in good agreement with each other but all of them are of the order of a few million degrees. The development of a reliable physical model for the mass and energy flow in the solar atmosphere depends critically on the knowledge of relevant heating and cooling mechanisms. One way of obtaining information about these mechanisms is through investigation of the physical conditions in the observed features of the solar structure characterized by different coronal magnetic field strength and configurations. From these studies, one can derive estimates of the energy in each region and thereby

obtain estimates of the required energy input. These estimates, combined with other information determined from the empirical and theoretical studies, provide insight into the possible heating mechanisms.

A number of observations were done to detect periodic oscillations or waves in the solar corona. Liebenberg and Hoffman found a 300 sec oscillation from their Concord observations obtained during the total solar eclipse of 1973 [2]. Soon after the acoustic-wave-heating models for the corona were discarded because of OSO-8 observations, and several theoretical studies emphasized the importance of looking for coronal waves in the shorter period range, some observations were carried out to search for these waves [3]. Pasachoff and Landman [4] and Pasachoff and Ladd [5] detected excess power in the 0.5-2 Hz range at level of 1 percent in the coronal green line. These observations were mostly confined at the green coronal line, using apertures with 2.5 and 5 arc sec diameters, isolating

¹ Present address: Physics Department, Damghan University of Sciences, Damghan
E-mail: reza5pm@yahoo.com

small regions of the solar corona. Meanwhile, Porter, Klimchuk, and Sturrock suggested that the fast magnetosonic waves may have the right flux and dissipation rate to overcome the radiation losses of the solar corona [6]. Singh and his colleagues prepared an observation to detect these waves during the total solar eclipse of 1995 in India, by fast photometry of a single location in the solar corona in continuum [7]. Results of this observation indicated oscillations in the frequency range 0.02-0.2 Hz with amplitudes between 0.2-1.3 percent of the coronal brightness. This team conducted another observation during the 1998 eclipse in Venezuela, with a six-channel photometer. They could detect intensity variations in the frequency range 0.01-0.2 Hz, with amplitudes in the range 0.5-3.5 percent of the coronal brightness, only in one channel [8].

From an analysis of the soft X-ray images taken with the Soft X-ray Telescope (SXT) on Yohkoh orbital observatory, Mckenzie and Mullan have also found the existence of waves with periods in the range 5-60 sec in the solar corona [9]. After that, a number of experiments conducted on-board solar and Heliospheric Observatory (SoHO) has given new insights into the physical and dynamical characteristics of the solar corona. The existence of the intensity and velocity oscillations, and the nature of these oscillations still need to be investigated because of their bearing on the mechanisms of the coronal heating. Among various kinds of waves, the fast mode waves undergo strong refraction due to the steep density gradient in the transition region, but may be important if generated in the corona itself. Transition Region And Coronal Explorer (TRACE) observations from 1998 have for the first time revealed the lateral displacements of the fast kink mode oscillations, with periods of 3-5 minutes, apparently triggered by the nearby flares and destabilizing filaments. Williams et al discovered fast oscillations with 6 s periods, which turned out to be propagating the fast magnetohydrodynamic (MHD) waves in a coronal loop [10]. Recently, Solar Ultraviolet Measurement of Emitted Radiation (SUMER) discovered with the Doppler shift measurements, the loop oscillations with longer periods (10-30 minutes) and relatively short damping times in hot (7 MK) loops, which seem to correspond to the longitudinal slow magnetoacoustic waves [11].

2. Observations

The last total solar eclipse of 20th century began in the North Atlantic about 300 Kilometers south of Nova Scotia where the moon's umbral shadow first touched down on the earth at 09:30:57 UT. The path of the moon's umbral shadow began in the Atlantic and crossed central Europe, the Middle East, and India where it finished at sunset in the Bay of Bengal. A good, clear and comfortable site is one of the most important parameters in an eclipse observation. Supply of the electricity, water, security and many other similar factors are also important in the site selection. After various

Table 1. The eclipse parameters at Esfahan (all times in UT).

Date	August 11, 1999
Julian Date	2451401.5
Radius of the Sun	15', 46.72"
Ephemeris transit time	12:05:14
Local transit time	13:13:48
First contact time	10:45
Fourth contact time	13:10
Maximum eclipse time	12:01:51
Totality duration	95 seconds

local inspections, we finally decided to set up our equipments inside Esfahan city (lat= 32°, 42' N, long= 50°, 38'E), at the Esfahan University campus, around 20 kilometers away from the center line. Some of the eclipse parameters are listed in Table 1.

There are many experiments that can be done during a total solar eclipse [12]. Our team conducted similar experiments during the 1995 and 1998 total solar eclipses [7,8]. We tried to examine our earlier observations on the fast photometry of the solar corona, to investigate the existence of oscillations, which may play a key role in the coronal heating mechanisms. A multichannel photomultiplier tube (PMT) was used to monitor six different (neighboring) regions in the solar corona. This multichannel photometer tube was specially designed and manufactured in the Indian Institute of Astrophysics, using six R647 photomultiplier tubes from Hamamatsu of Japan. Each channel received light from a small region of the corona, using a fiber optic with a length of about one meter and a 200 μm diaphragm. The end points of the fiber optics were assembled on a circular board with diaphragms, such that the distance of the nearest diaphragm from the center of the Sun was $1.2 R_{\odot}$, and the distance of the farthest one was $1.5 R_{\odot}$. The diaphragms were kept at the focal plate of the telescope. We used late Yohkoh soft X-ray images of the Sun to choose semi-active regions for our observations (unfortunately, Yohkoh lost its pointing due to an erroneous command during a solar eclipse in December 2001) [13]. A continuum filter with mean wavelength at $\lambda_0=4700 \text{ \AA}$ and passband of $\Delta\lambda= 190 \text{ \AA}$ was kept near the focal plate. All PMTs had been mounted in an aluminum box for magnetic and electric shielding to avoid the interference from nearby electronic circuits with the signal.

The diameter of the first mirror of the coelostat¹ was 30 cm. It tracked the sun with a stepper motor. The light

1. The abundance of light from the sun has frequently prompted the desire of studying it with a long-focus telescope, to produce an image of desirable size at its prime focus. Coelostat is such a device with two mirrors and an objective lens to make a completely fixed image of the sun (no motion or rotation). All modern solar observatories use coelostat as standard solar telescope.

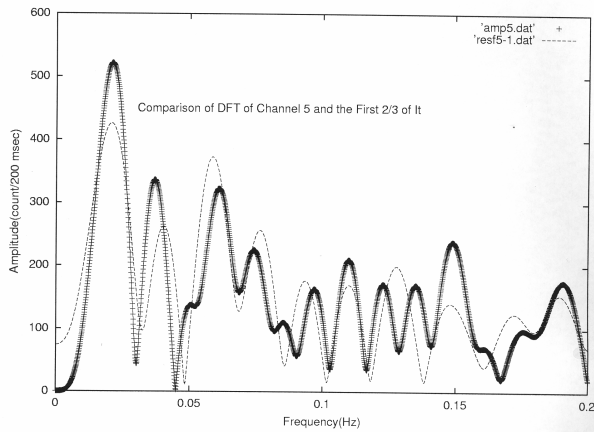


Figure 1. Piece-wise analysis: comparison of DFTs of channel5, and the first 2/3 of it. All channels show similar features as this.

path changed to the second mirror after reflecting from first mirror. Finally, it reached a Zeiss 20 cm doublet lens with 300 cm focal length (objective lens). The image scale on the focal plate was approximately 50000 Km/mm. Therefore, each fiber optic covered a circular region on the corona, with the diameter of about 10,000 km. In other words, each diaphragm aperture subtended an angle of 12 arc sec, which was much greater than the seeing level (~ 2 arc sec). So, the PMTs could only record variations when the waves in the region of interest were oscillating with some degree of coherence, giving a net oscillatory contribution to the intensity. The intensity of each PMTs was recorded at a rate of 5 Hz for all channels, using two lap top computers. About 90 seconds of the totality was observed in this experiment. We continued data recording a few seconds after the third contact. Dark data files were also recorded when the aperture was closed, a few minutes before the eclipse. The data acquisition were made using the software Quilet-9, developed by Prof. Edward Nather of University of Texas at Austin, USA, for the time series photometric study of the pulsating variables.

3. Data analysis

We tried to choose the reliable part of the data for each class of channels. The whole of the recorded data in all channels, around 90 seconds, were drawn for visual inspection. It was obvious that some chromospheric and photospheric light after the third contact had been recorded. After investigating these plots and comparing the first three channels with each other, we decided to take 86 seconds as completely reliable coronal data. Channel 6 failed to receive any coronal light. We discovered this problem a few days before the eclipse. Therefore, there was no time to re-assemble instruments to eliminate this problem. After comparing graphs of channels 4 and 5, we chose only 84 seconds of the data. We left channel 6 and continued analysis with the remaining five channels.

All of our data files show a parabolic trend. Coincidence of the minimum of the parabola with the

Table 2. General parameters of the observed oscillations in five channels.

Wave Number	Channel	Period(s)	Amplitude ¹
1	1	44.6 ± 2.2	0.65 ± 0.03
2	2	47.4 ± 2.3	0.57 ± 0.03
3	3	48.5 ± 2.3	0.47 ± 0.02
4	3	21.1 ± 1.0	0.30 ± 0.02
5	3	12.0 ± 0.6	0.29 ± 0.02
6	4	48.1 ± 2.3	0.39 ± 0.02
7	4	20.6 ± 1.0	0.31 ± 0.02
8	5	48.1 ± 2.3	0.45 ± 0.02
9	5	27.2 ± 1.3	0.29 ± 0.02
10	5	16.4 ± 0.8	0.28 ± 0.02

1. Amplitudes was presented in percent of the mean coronal brightness in the specified channel

maximum of the eclipse shows that this is just the scattered light in the atmospheric background during the eclipse time. To remove this effect from our data, we tried to subtract a polynomial from the original data. Thus, a residual file was obtained in each channel. The main test for the quality of the polynomial fit was clearance of the power spectrum, after trend subtraction. It is not easy to find the certain source for the scattered light. It may be due to cross talk between different optical components, as a possibility.

The Fourier analysis was applied to detect probable signals in our data. We calculated power spectrum for all channels. By visual inspection, similar features of some peaks were seen in all channels. To be more confident of the existence of these frequencies in the data, new data files were made by binning data over 2 and 5 points windows. These results were quite similar to original power spectrum. If all of oscillatory components identified in each channel were presented over the entire data length, a piece-wise analysis should yield similar features in their power spectrum. We divided each residual file into three parts and took the DFT (Discrete Fourier Transform) of the first, middle and last 2/3 of residual in each channel. All of these show almost the same features in amplitude spectrum with lower resolution, expected for their shorter data lengths, Figure 1. The shorter length of the subsets results in lower resolution power spectrum, thereby merging the nearby components. Nevertheless, it is clear that the amplitude spectrum of the subsets closely agree and the prominent peaks in the spectrum of the individual subseries are the same as the primary frequency components presented in each channel. To look for short-lived oscillations, we also did a piece-wise power spectrum analysis of the residuals. The DFT of much shorter subsets of the residuals were also derived (such as 1/5 of data). The resulting power spectrums did not show any significant components.

By a fine investigation of Table 2, we saw that some waves, for example 48.5 s, existed in more than one channel. Some other had small differences in their period, probably indicating the existence of these waves

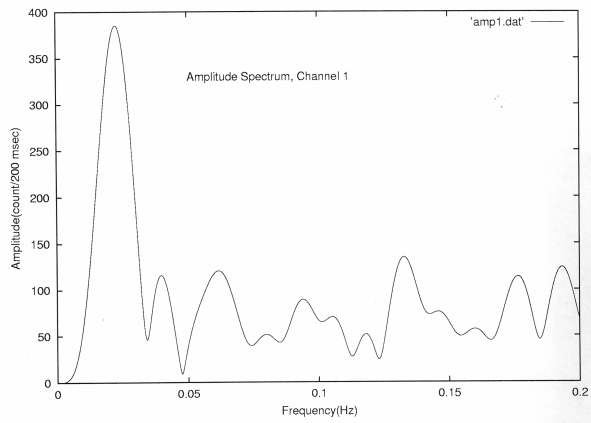


Figure 2. Amplitude Spectrum of Channel One.

in a great coronal region, larger than our PMTs window. Porter, Klimchuk, and Sturrock calculated damping length of the fast and slow MHD waves [6]. Their analysis suggests that only the fast mode damping scale height is of the order of a few hundred thousand kilometers. It may confirm our deduction for these waves being the fast mode magnetosonic waves. To double-check the presence of signal peaks in the amplitude spectrum, we used an auto correlation technique. At first, the auto correlation of residual files in all channels were taken and then their DFTs were calculated. Figure 2 is a sample of these DFTs. The threshold level for accepting a peak as a signal was 3σ . Finally all parameters of these high amplitude waves were obtained, using the Least-Squares method.

4. Spurious frequencies

In this part, we discuss and rule out the possibility of non-coronal oscillation mechanisms producing the above mentioned brightness modulations. We recorded dark and sky data before the eclipse. A close inspection of the DFT of the dark files indicates that there is no meaningful peak in the power spectrum. It means that probable noise frequencies in our detectors and electronic circuits are not in our interested range (up to 1 Hz). Figure (3), which is a plot of the power spectrum of the dark data of channel 3, clearly shows low amplitude peaks through out the entire frequency range. There is no concentration of the power at any frequency, especially at those frequencies appeared in our channels. These results rule out the possibility of the associated electronic modulation in the input brightness at all or some of the periodicities identified in the coronal data. The diaphragm of fiber optics covered an angle of about 12 arc sec in the sky and the brightness variation due to the effects of seeing, which could be in the range 2-3 arc sec, is expected to be small and random. The intensity variations due to the seeing effects usually lie in the frequency range 5-10 Hz, while all our observed frequencies, Table 2, are less than 1 Hz.

The gear system for driving the first mirror of the coelostat had also no periodicities comparable to the detected ones in Table 2. The stepper motor rotated once

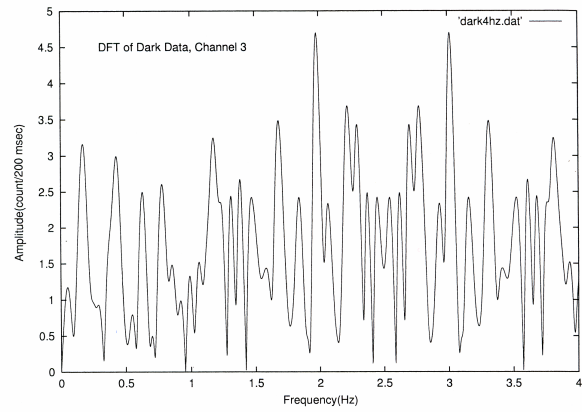


Figure 3. DFT of dark data do not show any concentration of power, especially in our detected frequencies.

in a second. Duration of steps of the stepper motor during the eclipse was 5255 μ sec and the next gear coupled to it rotated once in 420 seconds. The Coelostat mirror feeding the horizontal telescope rotated through an angle of 0.0375 arc sec every 5 msec in each step of the stepper motor, thereby producing an almost smooth tracking motion.

It was found visually that the continuous drift of the image could occur only because of the continuous change in declination of the Sun, which is negligible over 90 seconds. Hence, it is unlikely that the spatial variations in the corona coupled with the telescope pointing variation caused the above frequency components. The motion of coronal features is likely to produce non-sinusoidal and also non-periodic variations in the intensity.

The strong point in favor of attributing the above frequencies to the coronal oscillations is their extremely sinusoidal nature and near-coherence over the entire period of observation. We could determine their periods, amplitudes and input phases, which facilitated reconstruction of the data only because of these characteristics of the components. Furthermore, the harmonics of significant amplitudes were seen in the power spectrum. It is difficult to understand why any variation associated with either atmospheric transparency, or seeing effects, or image motion, or blurring should cause such coherent oscillation of constant amplitude over 90 sec interval. All above sources are expected to cause variations, but of non-periodic and variable amplitudes. Here, we stress that there is no reason to believe that the usual sources of error, most of which were considered above, could produce such a constant amplitude oscillations coherent over 90 seconds interval; any variation caused by them should be either random or spiky in nature. We conclude that the observed frequencies identified and given in Table 1 are not produced by any extraneous agencies, but are the essential components of the coronal brightness variation. The DFTs of final residuals were obtained after removing of the contribution from the

Table 3. Computed energy fluxes of the slow mode waves in the quiet and active regions.

No	Flux(quiet)	Flux(active)
1	7.9×10^3	1.0×10^3
2	7.0×10^3	9.0×10^3
3	5.7×10^3	7.5×10^3
4	3.7×10^3	4.8×10^3
5	3.2×10^3	4.1×10^3
6	4.8×10^3	6.2×10^3
7	3.8×10^3	4.9×10^3
8	5.5×10^3	7.1×10^3
9	3.5×10^3	4.6×10^3
10	3.4×10^3	4.4×10^3

Energy flux unit is (ergs cm⁻²s⁻¹).

mentioned frequencies in each channel. The height of the largest peak in this feature is much smaller than our detected signal peaks in the original power spectrum. Some peaks are in a doubtful level and we cannot comment on the realities of these peaks.

5. Energy fluxes of the waves

For a system to support oscillations, the size of the system must be equal or larger than the wavelength of oscillations. In the absence of spatial resolution required to discern these oscillations, one can surmise that there are regions with the size of the order of a wavelength and all these regions are oscillating with some degrees of coherence among them giving a net oscillatory contribution to the intensity. For estimating wavelengths of these oscillations, we supposed that the dimension of these regions are of the order of the wavelength of the oscillations. A thorough inspection of Table 2, confirms our guess. For example, there was a wave with frequency of about 0.02 Hz, which existed in all channels. This means that this wave existed in a region, bigger than the fiber optics dimensions.

We used a simple model to estimate the energy flux of the observed waves in our data, which is the energy density per unit volume times the propagation velocity. For the quiet Sun, we took the electron density $n_e = 5 \times 10^8$ cm⁻³, the magnetic field $B = 3$ G, and the electron temperature $T_e = 1.5 \times 10^6$ K. These parameters give the sound speed $C_S = 143$ kms⁻¹. Assuming that the observed oscillations are the slow mode, with a dispersion relation $\lambda = C_S P$, where P is the period of the waves, we estimated the energy flux of these oscillations as the slow mode waves in all channels, Table 3. The average wavelength of these slow mode waves in the quiet and active regions are 4800 km and 6200 km respectively, which is smaller than our PMTs aperture size, 10,000 km. Similarly, choosing the parameters of active regions as $n_e = 3 \times 10^9$ cm⁻³, the magnetic field $B = 100$ G, and the electron temperature $T_e = 2.5 \times 10^6$ K, gives

$C_S = 185$ kms⁻¹. The general flux formula is $F = \frac{1}{2} \rho_0 V_{\max}^2 V$ where V_{\max} is the maximum fluctuation velocity

Table 4. Computed energy fluxes of the fast mode waves in the quiet and active regions.

No	Flux(quiet)	Flux(active)
1	7.5×10^4	8.7×10^7
2	6.6×10^4	7.7×10^7
3	5.5×10^4	6.4×10^7
4	3.5×10^4	4.1×10^7
5	3.0×10^4	3.5×10^7
6	4.5×10^4	5.3×10^7
7	3.6×10^4	4.2×10^7
8	5.2×10^4	6.1×10^7
9	3.4×10^4	3.9×10^7
10	3.3×10^4	3.8×10^7

Energy flux unit is (ergs cm⁻² s⁻¹).

and V is the propagation velocity of the wave [14]. We estimated V_{\max} for the slow mode waves by $(\frac{\delta_0}{\delta_1}) C_S$

and for fast mode waves by $(\frac{\delta_0}{\delta_1}) V_A$, where $V_A =$

$\frac{B}{\sqrt{4\pi\rho}}$ is known as Alfvén velocity¹. So for the slow

mode waves, the energy flux is:

$$F = \frac{1}{2} \rho_0 \left(\frac{V_{\max}}{C_S} \right)^2 C_S^3 .$$

In this equation, $\rho_0 = n_e m_p$ is the mass density, and

$\left(\frac{\delta_1}{\delta_0} \right)^2 =$ amplitude of the intensity modulated and is

estimated by dividing the amplitude of the waves by the mean count of each channel.

For the fast mode waves, we also used the same relation to determine the energy flux. The dispersion relation for the fast mode is given as $\lambda = V_A P$. In this case, average wavelength in the quiet and active regions are 10,000 km and 59,000 km respectively. The same physical conditions were assumed for the quiet and active corona but the magnetic field were taken for the quiet and active regions equal to 2.4 G and 34 G, respectively. Assuming the magnetic field B to be the same for all the periods, we estimated the energy flux of them, for quiet and active regions, (Table 4). In this case, the energy flux for the fast mode waves is given by:

$$F = \frac{1}{2} \rho_0 \left(\frac{V_{\max}}{V_A} \right)^2 V_A^3 ,$$

where $V_{\max} = V_A \left(\frac{\delta_1}{\delta_0} \right)$.

¹ As C_S is the propagation speed of the sound waves, V_A is the characteristic propagation speed of MHD waves in a media (for more information on Alfvén, fast and slow mode waves in MHD see, for example, chapters five and six in reference [13]).

6. Conclusion

We conducted an experiment to detect high-frequency low-amplitude continuum intensity oscillations in the solar corona during the total solar eclipse, August 11, 1999 in Esfahan, Iran. Continuum filter with a mean wavelength at 4700 Å was used to do photometric observation. The photometric data were recorded at a rate of 5 Hz. There were some coronal intensity oscillations of periods ranging from 12 to 48 seconds. The amplitude of these waves were 0.3-0.7 percent of mean coronal brightness. A piece-wise analysis indicated that these waves were presented in the whole observation time. The Fourier transform and auto correlation technique were applied to investigate the presence of the signals in our data. The energy flux of these waves was calculated as the slow or fast mode waves in the active and quiet regions of the solar corona. If these oscillations are identified with the fast magnetosonic mode, they provide enough energy flux for heating up both the quiet and active regions in the solar corona. Results of this experiment demonstrate that these waves are present in a

large coronal region, larger than the PMTs windows. So, the damping length of them may be of the order of a few hundred thousand kilometers. More complementary 2D experiments are needed to investigate the damping rate and mechanisms of these waves. Simultaneous measurements of the coronal magnetic field may help also.

Acknowledgments

We wish to thank Dr. Mehdi Jahan Miri and Mr. Iraj Gholami, who helped us in managing the eclipse observation. We gratefully acknowledge Prof. Y. Sobouti and Dr. M.R.H. Khajepour from the Institute for Advanced Studies in Basic Sciences (IASBS) for their kind collaboration and supporting the project. This work was partly supported by the Indian Institute for Astrophysics (IIA), Bangalore, India. Finally, we thank prof. Edward Nather of University of Texas at Austin, USA for permitting us to use the data acquisition software "Quilt-9".

References

1. A N Cox, W C Livingston and M S Matthews, *Solar Interior and Atmosphere* (1991).
2. D H Leibenberg and M M Hoffman, *Coronal Disturbances*, in G. Newkirk(ed), IAU Symp. **57**(1974) 485.
3. J A Ionson, *Astrophys. J.* **226**(1978) 650.
4. J M Pasachoff and D A Landman, *Solar Phys.* **90**(1984) 325.
5. J M Pasachoff and E D Ladd, *Solar Phys.* **109**(1987) 365.
6. L J Porter, J A Klimchuk and P A Sturrock, *Astrophys. J.* **435**(1994)482.
7. J Singh, et al., *Solar Phys.* **170**(1997)235.
8. R Cowsik, J Singh, A K Saxena, R Sirinivasan and A V Raveendran, *Solar Phys.* **188**(1999)89.
9. D E Mackenzie and D J Mullan, *Solar Phys.* **176**(1998)127.
10. D R Williams, et al., *MNRAS*, **326**(2001)428.
11. M J Aschwanden, *Turbulence, Waves and Instabilities in the Solar Plasma, NATO Science Series : II: Mathematics, Physics and Chemistry.* (eds. R Erdelyi, K Petrovay, B Roberts and M J Aschwanden), Kluwer Academic Publishers, NATO Advanced Research Workshops, (16-20 Sept 2002), Budapest, Hungary.
12. J Singh, *Bull. Astr. Soc. India*, **22**(1994)339.
13. M J Aschwanden, *Physics of the Solar Corona: An Introduction* (2004) Springer-Praxis.
14. R G Athay, O R White, *Astrophys. J.*, **39**(1978)333.